Construction of the particle simulation model for ginger-soil system using discrete element method

Wenlong Wang[1†], Pengcheng Zhang[1,2†], Xin Wang[3], Xiaojun Meng[1*], Fangyan Wang[1,2*]

(1. *College of Mechanical and Electrical Engineering, Qingdao Agricultural University, Qingdao 266109, Shandong, China*;
2. *Collaborative Innovation Center for Shandong's Main Crop Production Equipment and Mechanization, Qingdao 266109, Shandong, China*;
3. *College of Civil Engineering & Architecture, Qingdao Agricultural University, Qingdao 266109, Shandong, China*)

Abstract: In order to systematically obtain the excavation characteristic parameters for ginger harvesting, experimental analysis was conducted on the discrete elemental parameters in a particle simulation model of the ginger-soil system. Through stacking tests, the surface energy of soil-ginger tuber JKR was determined to be 3.7 J/m^2, the coefficient of static friction of soil-steel (65 Mn) was 0.56, the coefficient of rolling friction was 0.03, and the coefficient of restitution of collision was 0.40. Utilizing normal and lateral compression tests conducted on the soil body, the soil base parameters required for the Bonding model were determined. Subsequently, a three-dimensional model of ginger root and stem was constructed using these parameters. With the aid of 3D scanning technology, a discrete element parameter model was established for the ginger field during the harvesting period. On the basis of the measured parameters, a three-dimensional model of ginger rhizome was established and finally a discrete parameter model of ginger field was constructed in the harvesting period. The calibration parameters are highly reliable after the model's tightness and field harvesting test, which provides reliable data support for the soil flow and the force of the soil-touching parts during the later simulation of ginger harvesting and digging operation.

Keywords: ginger, soil, discrete element, simulation parameters, calibration
DOI: 10.25165/j.ijabe.20241705.9102

Citation: Wang W L, Zhang P C, Wang X, Meng X J, Wang F Y. Construction of the particle simulation model for ginger-soil system using discrete element method. Int J Agric & Biol Eng, 2024; 17(5): 58–64.

1 Introduction

Ginger holds significant importance in China as an essential export commodity and a significant source of foreign exchange earnings. China boasts the largest ginger planting area globally. Nevertheless, the mechanized harvesting of ginger faces challenges with low efficiency, elevated digging resistance, and susceptibility to ginger piece damage. Through the use of discrete element simulation technology, the key to optimizing the ginger harvesting equipment and improving the level of mechanized harvesting lies in exploring the motion laws, encompassing aspects such as soil load and deformation, as well as ginger load and motion dynamics throughout the ginger harvesting process[1-5]. At present, the main focus of discrete element simulation technology has centered on the parameter calibration of corn, wheat and other seeds, as well as the construction of granular body models[6-8]. The discrete element-based granular body simulation model was constructed by determining the essential parameters (density, shear modulus, Poisson's ratio, and others) for the crops. Additionally, contact parameters (surface energy between particles, between particles and the surrounding materials, coefficient of restitution, coefficient of static friction, coefficient of rolling friction, and others) were determined and incorporated into the model[9]. Due to the difference between the granular body and the actual crop, there are difficulties in obtaining an accurate granular body simulation model by relying only on the directly determined parameters[10]. The current discrete element models for root crop harvesting are lacking in ability with regard to accurately simulating the soil's water content and adhesion characteristics. Zhang et al.[11] made a notable improvement to the traditional discrete element model by incorporating the effects of liquid bridge force and adhesion force between soil particles. This modification significantly enhanced the model's ability to produce simulation results that closely resemble real-world conditions. However, the soil model is homogeneous and lacks a representation of crops, making it incapable of simulating crop loading and the effects of soil fragmentation. At the same time, parameters such as water content and critical stress are affected by soil depth, and soil discrete element model parameters need to be determined and established in layers[12-14]. In particular, the high water content and complex particle composition of the soil during the ginger harvesting period require a virtual calibration method to obtain relatively accurate calibration parameters[15,16]. Currently, there is a scarcity of research on ginger modeling and particle body simulation modeling of the ginger-soil system. As such, in line with the methodology employed for crop parameter determination, discrete elemental parameter calibration was conducted for ginger tubers and soil during the harvesting period. On the basis of the existing research, this paper takes the soil planted with cotton ginger

Received date: 2024-05-29 **Accepted date:** 2024-09-09
Biographies: Wenlong Wang, MS candidate, research interest: agricultural machinery and equipment, Email: 1315378398@qq.com; **Pengcheng Zhang**, MS, research interest: agricultural machinery and equipment, Email: 1258767989@qq.com; **Xin Wang**, PhD, Lecturer, research interest: solid mechanics and its applications, Email: betty_wx@126.com.
†These authors contributed equally to this work.
***Corresponding author: Xiaojun Meng**, PhD, Professor, research interest: design and theory of agricultural equipment. College of Mechanical and Electrical Engineering, Qingdao Agricultural University, Qingdao 266109, Shandong, China. Tel: +86-13515385935, Email: mxj931@qau.edu.cn; **Fangyan Wang**, PhD, Professor, research interest: design and theory of agricultural equipment. College of Mechanical and Electrical Engineering, Qingdao Agricultural University, Qingdao 266109, Shandong, China. Tel: +86-15806426016, Email: wfy_66@163.com.

as an example. The soil is loam with higher moisture content and greater viscosity, and analyzes the discrete element parameters of the soil in the harvest period of ginger field. This effort aimed to establish a granular body simulation model for the ginger-soil system, thereby offering a modeling framework for the investigation of factors contributing to ginger damage and the reasons behind high excavation resistance[17,18].

2 Calibration of contact parameters for ginger-soil systems

The In the present study, the intrinsic parameters of the ginger-soil system were measured experimentally. The determination of contact parameters between soil particles and ginger, such as JKR surface energy parameters, collision recovery coefficients, static friction coefficients, and rolling friction coefficients, was achieved through a combination of methods including the steepest-climbing test, the Box-Behnken test, and regression analysis of variance (ANOVA). These approaches are beneficial in identifying the optimal parameter combinations for soil particles and ginger in the simulation model. The characteristic parameters of soil and ginger were determined by means of data searching as well as tests, as listed in Table 1. Using EDEM's own particle unit, Single Sphere, Straight Four, Square Four, and Triple Sphere were utilized to establish soil spherical block particles, columnar particles, block particles, and nuclear particles, respectively, as shown in Figure 1[18-21].

Table 1 Data on soil contact parameters in ginger fields

Parameter	Value	Parameter	Value
Density of soil particles/kg·m^{-3}	2680	Poisson's ratio of ginger particles	0.28
Soil particle shear modulus/MPa	1	Soil-soil surface energy/J·m^{-2}	3.53
Poisson's ratio of soil particles	0.38	Soil-soil coefficient of restitution	0.31
65 Mn density/kg·m^{-3}	7861	Soil-soil coefficient of static friction	0.68
65 Mn shear modulus/Pa	7.9×10^{10}	Soil-soil coefficient of rolling friction	0.05
65 Mn Poisson's ratio	0.28	Soil-65 Mn steel coefficient of restitution	0.44
Ginger particle density/kg·m^{-3}	1160	Soil-65 Mn steel coefficient of static friction	0.45
Ginger particle shear modulus/MPa	1.21	Soil-65 Mn steel coefficient of rolling friction	0.12

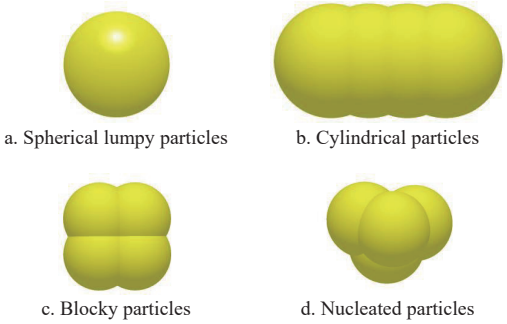

a. Spherical lumpy particles b. Cylindrical particles

c. Blocky particles d. Nucleated particles

Figure 1 Soil particle model

2.1 Steepest climb test

Through the use of the GEMM database in EDEM, the range of values of contact parameters (JKR surface energy parameter, coefficient of restitution, coefficient of static friction and coefficient of rolling friction of soil particles and ginger) was obtained. These values were derived from the steepest climb test[22] results, and the mixing angle of repose, as illustrated in Figure 2, was set at 34.43°, as detailed in Table 2. As the values of factors A, B, C, and D increased, the stacking angle derived from the simulation gradually increased, and the relative error between the simulation results and the actual values exhibited a tendency to decrease and then increase. The relative error of the stacking angle reached the minimum value at the No. 2 test level. Therefore, the No. 2 level was selected as the center point and set as the medium level, and the No. 1 and No. 3 levels were selected as the low and high levels, respectively.

Figure 2 Mixed soil and tuber stacking test

Table 2 Steepest climb test program and results

Serial number	Parameter A/(J·m^{-2})	Parameter B	Parameter C	Parameter D	Angle of repose/(°)	Relative error/%
1	3.50	0.15	0.20	0	33.21	3.55
2	6.13	0.30	0.44	0.05	34.16	0.78
3	7.75	0.45	0.68	0.10	39.62	15.07
4	11.38	0.60	0.92	0.15	41.63	20.92
5	14.00	0.75	1.16	0.20	45.51	32.18

Note: Parameters A, B, C, and D refer to the JKR surface energy parameter, coefficient of restitution, coefficient of static friction, and coefficient of rolling friction, respectively, between soil particles and ginger tubers.

2.2 Box-Behnken test

The Box-Behnken test method was selected in the present study, and the experimental design scheme and results are listed in Table 3. Through the utilization of Design-Expert software, the effect of each factor on the angle of repose of soil φ was determined, and by excluding factors that did not have a significant effect on the accumulation angle, the second-order regression equation could be obtained as:

$$\varphi = 37.42 + 6.79A - 5.39B + 6.08D - 7.56AB + 7.74AC + 8.04AD + 9.84BC - 7.86BD + 12.12C^2 \quad (1)$$

In this regression simulation equation, the effects of factor C and the interaction terms CD, A^2, B^2, and D^2 on angle of repose were not significant. From the one-factor level analysis, an observation can be made that the order of magnitude of the effect of each factor on the angle of repose was $A>D>B>C$; in the interaction, $BC>AD>BD>AC>AB>CD$; $C^2>A^2>B^2>D^2$, as listed in Table 4.

2.3 Analysis of factor interaction effects

By employing Design-Expert software, the response surface plots of the effect of each factor on the index were derived. From Figure 3, an observation can be made that the angle of repose exhibited a gradual increase with the increase in JKR surface energy; with the increase in collision recovery coefficient, the angle of repose exhibited a decreasing trend under the interaction with the static friction coefficient; the angle of repose gradually increased with the increase in rolling friction coefficient; and the angle of repose firstly decreased and then gradually increased with the increase in static friction coefficient.

2.4 Optimal parameter combination and simulation verification

Utilizing the Design-Expert software, optimization was conducted under the condition of a mixed angle of repose set at 34.43°. The resulting optimized values for the JKR surface energy

Table 3 Box-Behnken experimental design scheme and results

Serial number	Parameter A/J·m^{-2}	Parameter B	Parameter C	Parameter D	Angle of repose/(°)
1	0(5.63)	0(0.30)	0(0.44)	0(0.05)	38.97
2	0	−1(0.15)	0	1(0.10)	43.41
3	0	0	−1(0.20)	−1(0)	30.27
4	−1(3.50)	1(0.45)	0	0	23.42
5	1(7.75)	0	−1	0	47.89
6	0	0	0	0	25.57
7	0	0	0	0	38.43
8	0	−1	−1	0	70.56
9	0	1	−1	0	30.16
10	0	−1	1(0.68)	0	46.45
11	0	1	0	1	30.49
12	0	1	1	0	45.41
13	−1	−1	0	0	22.72
14	1	−1	0	0	51.55
15	0	0	0	0	43.47
16	0	0	0	0	40.69
17	0	0	−1	1	55.74
18	−1	0	0	−1	28.96
19	−1	0	0	1	26.26
20	0	0	1	1	53.93
21	−1	0	−1	0	46.01
22	0	−1	0	−1	22.68
23	0	0	1	−1	43.29
24	1	0	0	−1	22.59
25	1	0	0	1	52.05
26	1	0	1	0	63.39
27	0	1	0	−1	41.18
28	1	1	0	0	22.01
29	−1	0	1	0	30.56

Table 4 Box-Behnken test quadratic model ANOVA

Source	Sum of squares	Degrees of freedom	Mean square	*F*-value	*p*-value	Significance
Model	4092.05	14	292.29	5.91	0.0010	Significant
A	554.06	1	554.06	11.21	0.0048	Significant
B	348.88	1	348.88	7.06	0.0188	Significant
C	0.4784	1	0.4784	0.0097	0.9230	not Significant
D	443.07	1	443.07	8.96	0.0097	Significant
AB	228.61	1	228.61	4.62	0.0495	Significant
AC	239.43	1	239.43	4.84	0.0451	Significant
AD	258.51	1	258.51	5.23	0.0383	Significant
BC	387.2	1	387.2	7.83	0.0142	Significant
BD	246.82	1	246.82	4.99	0.0423	Significant
CD	55.04	1	55.04	1.11	0.3093	not Significant
A^2	86.93	1	86.93	1.76	0.2061	not Significant
B^2	28.07	1	28.07	0.5677	0.4637	not Significant
C^2	953.12	1	953.12	19.28	0.0006	Significant
D^2	25.39	1	25.39	0.5135	0.4854	not Significant
Residual	692.22	14	49.44			
Lack of fit	501.06	10	50.11	1.05	0.5269	not Significant
Pure error	191.16	4	47.79			
Cor total	4781.27	28				

parameter for the soil-ginger interface were determined to be 3.7 J/m^2, with corresponding coefficients of restitution, rolling friction, and static friction at 0.40, 0.56, and 0.03, respectively. The results of the simulation test of the stacking of ginger and soil under the optimal combination of the solution parameters are shown in Figure 4. The simulation test yielded a result of 35.26°, which is highly similar to the real test result, and the relative error was 2.41%, which could be used for the calibration of the model contact parameters.

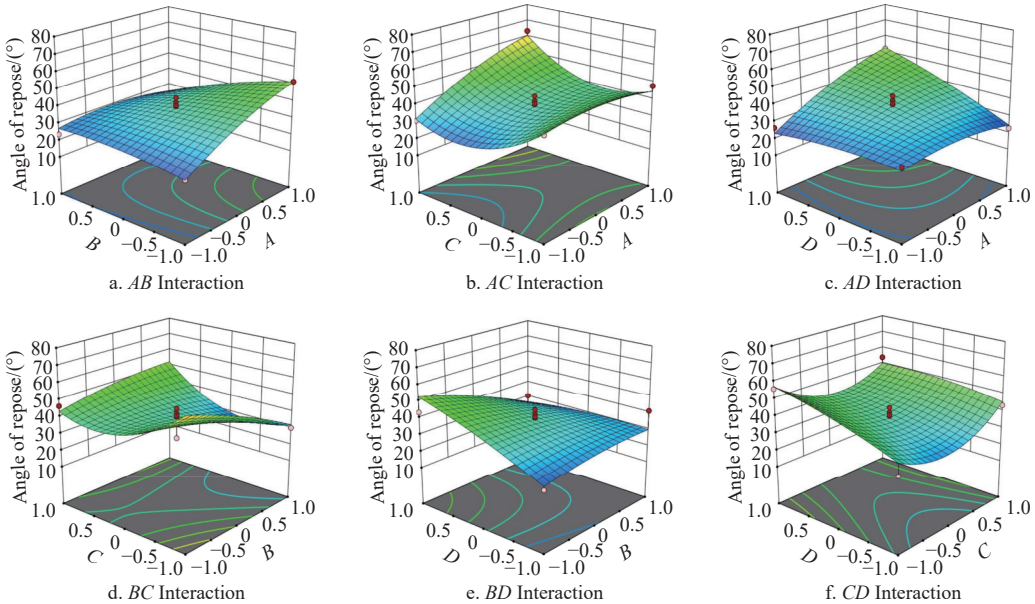

a. *AB* Interaction b. *AC* Interaction c. *AD* Interaction

d. *BC* Interaction e. *BD* Interaction f. *CD* Interaction

Figure 3 Interaction between influencing factors

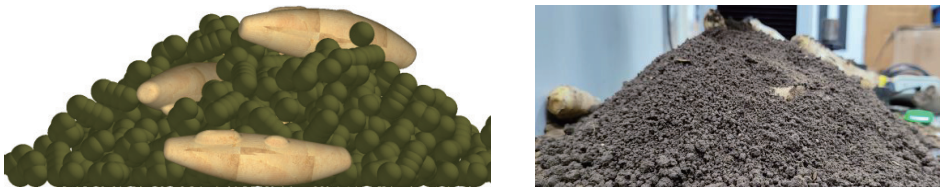

a. Simulation test b. Physical test

Figure 4 Comparison of simulation and physical test results

3 Establishment of soil mechanical modeling parameters

3.1 Determination of contact radius of soil particles

Upon conducting a thorough investigation, it was ascertained that the dimensions for ginger cultivation exhibited specific ranges, as follows: the width of ginger border B=650-700 mm, the width of ginger ridge b=350-450 mm, the depth of the tuber from the bottom of ditch h_1=150-200 mm, and the height of ridge h_2=250-300 mm. Considering the variability of growth in the field, B=700 mm, b=350 mm, h_1=150 mm, and h_2=300 mm were chosen. The condition of the ginger field in harvesting period is shown in Figure 5.

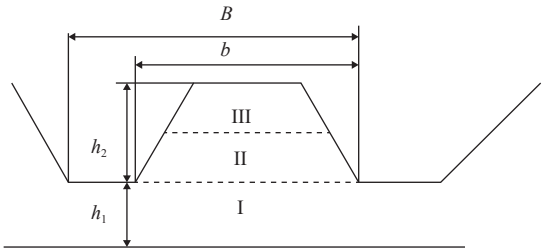

Figure 5 Cross-section of ginger field division during harvesting period

Due to multiple soil cultivation activities contributing to the formation of ginger ridges, it was observed that the soil quality remained relatively consistent from the top to the bottom of these ridges. Typically, the surface layer tended to be loose, while the underlying layer exhibited increased hardness. Additionally, the bottom of the furrow became hardened due to repeated soil cultivation operations. To ensure the accuracy of the model, a stratified sampling approach was employed for ginger ridges, acknowledging these variations in soil characteristics at different layers within the ridges. Taking the bottom of ginger tuber growth as the benchmark, it was divided into Ⅰ, Ⅱ, and Ⅲ zones from the bottom up. The soil density was determined by weighing after sampling using the ring knife method. Through the utilization of a soil tester and a DHS-16A moisture tester, soil compactness and water content were determined with reference to the GB5009.3-2016 determination method[23].

Soil has a complex structure and consists mainly of soil particles and water. The water content plays a crucial role in influencing the interactions and bonding between soil particles, conforming to the relationship described by Equation (2).

$$\frac{m_1}{m}=\frac{\rho_{\text{water}}v_{\text{water}}}{\rho_{\text{soil}}v_{\text{soil}}+\rho_{\text{water}}v_{\text{water}}}=x\% \tag{2}$$

where, m_1 is the mass of moisture, kg; m is the total mass of the specimen, kg.

Set the soil, soil particles and water volume as $v_{\text{soil}}=\frac{4}{3}\Pi R_1^3$, $v_{\text{water}}=\frac{4}{3}\Pi R_2^3-\frac{4}{3}\Pi R_1^3$, and the radius of soil particles is taken as R_1=6 mm, the density of soil particles is taken as 2680 kg/m^3[18], then the cohesive radius of the particles in the soil model, R'_1[24], can be denoted as listed in Table 5.

Table 5 Soil particle bonding radius parameters

Region	Moisture content/%					Bonded Disk Radius/mm				
	Maximum value	Minimum value	Mean value	Standard deviation	Coefficient of variation	Maximum value	Minimum value	Mean value	Standard deviation	Coefficient of variation
Ⅰ	12.97	9.29	10.80	1.15	0.11	6.34	5.89	6.08	0.220	0.04
Ⅱ	14.87	10.25	11.99	1.65	0.14	6.39	5.85	6.13	0.222	0.04
Ⅲ	14.62	8.96	12.03	2.37	0.20	6.07	5.64	5.87	0.214	0.04

3.2 Determination of bonding parameters of soil particles

The soil was tested in compression using a universal tester to determine the critical stress. A standard cylindrical specimen (39.1 mm in diameter and 80 mm in height) was fabricated. The testing protocol involved applying a loading rate of 10 mm/min[25] to the specimen until it either ruptured, slipped, or disintegrated completely. Throughout the testing procedure, the variations in stress and displacement values were meticulously recorded and monitored, as shown in Figure 6.

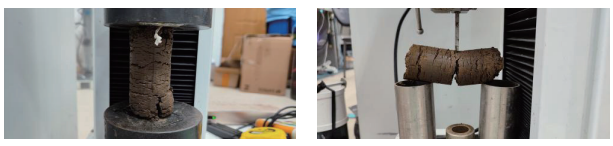

a. Soil normal compression damage b. Soil tangential compression damage

Figure 6 Soil compression test

Through the compression test, the stress versus deformation curves were measured to obtain the Critical Normal Stress and Critical Shear Stress of the soil body, that is, the maximum bond normal and tangential stresses of the soil model. From Equation (3), the Stiffness per unit area of the soil body was obtained, as listed in Tables 6 and 7[26-29].

$$\begin{aligned}\delta F_n&=-V_nS_nA\delta_t\\ \delta F_t&=-V_tS_tA\delta_t\end{aligned} \tag{3}$$

where, S_n is normal stiffness per unit area of soil, N/m^3; S_t is shear stiffness per unit area of soil, N/m^3; V_n and V_t are speeds under load, m/s; A is cross-sectional area, m^2; δ_t is loading time, s.

3.3 Particle simulation model construction and validation of ginger-soil system

Utilizing 3D scanning technology, ginger tubers were scanned and modeled as shown in Figure 7. The results of ginger and soil parameter measurements during the harvest period are shown in Table 8. The particle radius was set as 6 mm, the particle simulation model of the ginger-soil system in the harvest period was established, and tightness puncture simulation testing was conducted[30-33], as shown in Figure 8. The measurement data are shown in Table 9. In conjunction with the mechanized ginger harvesting process, specific operational parameters were applied during field testing of the ginger digging and shaking device. These parameters included forward speed V_m=0.3 m/s, shovel surface inclination angle a=15°, judder frequency f=4.2 Hz, and tilting angle of shaking fence β_0=26°[34-37]. The results of both the field test and simulation test are presented in Figure 9, and the measured data are shown in Table 10. Through data comparison, findings were made that in the tightness puncture test, the simulation parameter test value was slightly larger than the actual value, and the maximum error of the data was 7.95%. In the field harvesting overall effect comparison, where the machine covered a distance of 80 m per test run (15 m in the preparation area, 50 m in the test area, and 15 m in the adjustment area) across 10 trials, the analysis

Table 6 Parameters of soil bonding stress in ginger field

Region	Critical normal stress/MPa					Critical shear stress/MPa				
	Maximum value	Minimum value	Mean value	Standard deviation	Coefficient of variation	Maximum value	Minimum value	Mean value	Standard deviation	Coefficient of variation
I	0.45	0.19	0.28	0.09	0.34	0.22	0.08	0.12	0.0550	0.47
II	0.14	0.03	0.09	0.04	0.45	0.01	0.01	0.01	0.0020	0.16
III	0.09	0.02	0.05	0.03	0.59	0.01	0.01	0.01	0.0009	0.11

Table 7 Parameters of soil bond stiffness in ginger fields

Region	Normal stiffness per unit area/N·m^{-3}					Shear stiffness per unit area/N·m^{-3}				
	Maximum value	Minimum value	Mean value	Standard deviation	Coefficient of variation	Maximum value	Minimum value	Mean value	Standard deviation	Coefficient of variation
I	42 444 821.73	18 270 987.59	28 561 591.93	8 448 451.36	0.30	26 540 284.36	6 553 079.95	13 040 881.80	7 602 939.26	0.58
II	50 724 637.68	7 260 406.58	27 800 242.55	15 480 848.76	0.56	7 776 049.77	5 602 240.90	6 557 270.19	978 962.70	0.15
III	25 157 232.70	6 107 669.49	16 392 709.27	7 842 272.61	0.48	6 516 072.98	4 467 277.20	5 314 555.88	1 069 347.79	0.20

Figure 7 3D scanning modeling of ginger

Table 8 Discrete elemental contact parameters of ginger field

Parameter	Numerical value	Parameter	Numerical value
Density of soil particles/kg·m^{-3}	2680	Soil-soil coefficient of restitution	0.31
Soil particle shear modulus/MPa	1	Soil-soil coefficient of static friction	0.68
Poisson's ratio of soil particles	0.38	Soil-soil coefficient of rolling friction	0.05
65 Mn steel density/kg·m^{-3}	7861	Soil-65 Mn steel coefficient of restitution	0.44
65 Mn steel shear modulus/Pa	7.9×10^{10}	Soil-65 Mn steel coefficient of static friction	0.45
65 Mn steel Poisson's ratio	0.28	Soil-65 Mn steel coefficient of rolling friction	0.12
Ginger particle density/kg·m^{-3}	1160	Soil-ginger surface energy/J·m^{-2}	3.70
Ginger particle shear modulus/MPa	1.21	Soil-ginger coefficient of restitution	0.40
Poisson's ratio of ginger particles	0.28	Soil-ginger coefficient of static friction	0.56
Soil-soil surface energy/J·m^{-2}	3.53	Soil-ginger coefficient of rolling friction	0.03

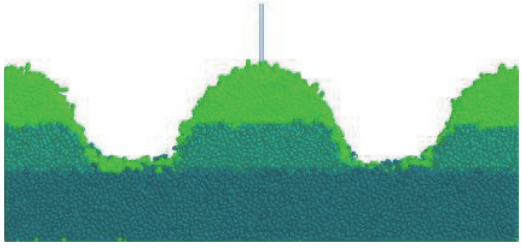

Figure 8 Discrete element model of ginger field

Table 9 Comparison of tightness parameters

Region	Tightness/MPa (simulated value)	Tightness/MPa (test value)	Relative error/%
I	1.98	1.92	3.13
II	1.46	1.41	3.55
III	0.95	0.88	7.95

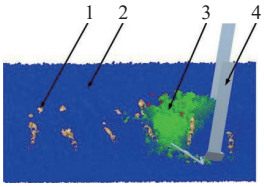

1. Ginger tuber 2. Soil particles
3. Soil congestion
4. Digging and shaking device

a. Simulated excavation test

b. Field test excavation

Figure 9 Excavation calibration test

Table 10 Comparison of forward resistance

Serial number	Analog value/N	Measured value/N	Relative error/%
1	1501.29	1458.44	2.94
2	1473.50	1447.81	1.77
3	1320.17	1327.50	0.55
4	1574.40	1406.25	11.96
5	1553.03	1423.44	9.10
6	1468.74	1693.13	13.25
7	1589.54	1391.88	14.20
8	1533.43	1722.81	10.99
9	1486.88	1506.25	1.29
10	1483.79	1551.25	4.35
Mean value	1498.48	1492.88	0.38
Standard deviation	75.95	128.95	
Coefficient of variation	0.05	0.09	

of the average forward resistance during ginger harvesting in the test area[38] revealed a maximum relative error of approximately 14.20%. The error value was relatively small, primarily stemming from the complex harvesting conditions encountered during the field tests. Through data analysis, the feasibility and accuracy of the particle simulation model of ginger-soil system were verified, thereby providing theoretical data support for the subsequent design.

4 Discussion

The angle of repose was obtained through stacking test, and the steepest climb test and the Box-Behnken test were conducted to derive calibrated values for the pertinent contact parameters. The JKR surface energy between soil particles is slightly smaller relative to the values between soil particles and ginger tubers, which indicates that it is more difficult for the soil to detach and adhere to the tubers during the actual field harvesting process, in line with the state of ginger tubers that have a larger soil content during the actual harvesting process.

The compression test conducted on soil samples utilizing a universal tester provided critical parameters related to the soil's behavior. According to the determination of soil water content, the soil particle contact radius parameters were obtained. The soil-ginger system was modeled by combining the measured parameters.

The modeling process primarily accounted for moisture as the key factor influencing the adhesion between soil particles, neglecting the impact of gas and other factors. Meanwhile, the pertinent contact parameters were determined only for cotton ginger, not for other varieties of ginger. The computational accuracy of the particles can be improved during subsequent simulations.

5 Conclusions

1) Following the stacking test, the angle of repose for the soil-ginger mass mixture during harvest was determined to be 34.43°. Through the simulation tests and the control of physical test, the finalized soil-ginger tuber JKR surface energy was 3.7 J/m^2; the soil-steel (65 Mn) coefficient of static friction was 0.56, the coefficient of rolling friction was 0.03, and the coefficient of static friction was 0.40.

2) Compression tests on soil samples with the aid of a universal tester yielded soil Zone I - the Bonded Disk Radius was measured at 6.08 mm, accompanied by a Critical Normal Stress of 0.28 MPa, a Critical Shear Stress of 0.12 MPa, Normal Stiffness per unit area at 2.856×10^7 N/m^3, and Shear Stiffness per unit area at 1.304×10^7 N/m^3; Zone II - the Bonded Disk Radius was found to be 6.13 mm, with a Critical Normal Stress of 0.09 MPa, a Critical Shear Stress of 0.01 MPa, Normal Stiffness per unit area of 2.78×10^7 N/m^3, and Shear Stiffness per unit area of 6.557×10^6 N/m^3; Zone III-the Bonded Disk Radius was measured at 5.87 mm, accompanied by a Critical Normal Stress of 0.053 MPa, a Critical Shear Stress of 0.008 MPa, Normal Stiffness per unit area at 1.639×10^7 N/m^3, and Shear Stiffness per unit area at 5.315×10^6 N/m^3.

3) Comparing the simulated and experimental values of ginger field compactness, both of them increased with increasing depth, with a maximum error of 7.95%. The error between the forward resistance of the field digging operation and the simulation calculation was about 14.20%, which was small and mainly originates from the complexity of the harvesting environment. This proves the accuracy and reliability of the modeling, and provides support for the subsequent motion analysis of the digging components for ginger harvesting. This proves the accuracy and reliability of the modeling, and provides support for the subsequent motion analysis of the excavation components for ginger harvesting.

Acknowledgements

This study was supported by the National Natural Science Foundation of China (Grant No. 52275258), the Taishan Scholar Youth Expert Project (Grant No. tsqn202306243), and the Open Fund of Collaborative Innovation Center for Shandong's Main Crop Production Equipment and Mechanization (Grant No. SDXTZX-10).

[References]

[1] Huang Y X, Hang C G, Yuan M C, Wang B T, Zhu R X. Discrete element simulation and experiment on disturbance behavior of subsoiling. Transactions of the CSAM, 2016; 47(7): 80–88. (in Chinese)

[2] Lenaerts B, Aertsen T, Tijskens E, Ketelaere B D, Ramon H, Baerdemaeker J D, et al. Simulation of grain-straw separation by Discrete Element Modeling with bendable straw particles. Computers and Electronics in Agriculture, 2014; 101: 24–33.

[3] Zhang Z G, Zeng C, Xing Z Y, Xu P, Guo Q F, Shi R M, et al. Discrete element modeling and parameter calibration of safflower biomechanical properties. Int J Agric & Biol Eng, 2024; 17(2): 37–46.

[4] Wang Y X, Liang Z J, Cui T, Zhang D X, Qu Z, Yang L. Design and Experiment of Layered Fertilization Device for Corn. Transactions of the CSAM, 2016; 47(S1): 163–169. (in Chinese)

[5] Zhang X J, Wang H T, Wang F Y, Lian Z G. Parameter calibration of discrete element model for alfalfa seeds based on EDEM simulation experiments. Int J Agric & Biol Eng, 2024; 17(3): 33–38.

[6] Coetzee C J, Els D N J. Calibration of discrete element parameters and the modelling of silo discharge and bucket filling. Computers and Electronics in Agriculture, 2008; 65(2): 198–212.

[7] Cunha R N, Santos K G, Lima R N, Duarte C R, Barrozo M A S. Repose angle of monoparticles and binary mixture: An experimental and simulation study. Powder Technology, 2016; 303: 203–211.

[8] Shi L R, Zhao W Y, Sun B G, Sun W, Zhou G. Determination and analysis of basic physical and contact mechanics parameters of quinoa seeds by DEM. Int J Agric & Biol Eng, 2023; 16(5): 35–43.

[9] Wang L J, Li R, Wu B X, Wu Z C, Ding Z J. Determination of the coefficient of rolling friction of an irregularly shaped maize particle group using physical experiment and simulations. Particuology, 2018; 38: 185–195.

[10] Wang X L, Hu H, Wang Q J, Li H W, He J, Chen W Z. Calibration Method of Soil Contact Characteristic Parameters Based on DEM Theory. Transactions of the CSAM, 2017; 48(12): 78–85. (in Chinese)

[11] Zhang R. Research on the dynamic behavior of soil based on mesocopic simulation by distinct element method. Jilin University, 2005. (in Chinese)

[12] Yang Q Z, Shi L, Shi A P, He M S, Zhao X Q, Zhang L, et al. Determination of key soil characteristic parameters using angle of repose and direct shear stress test. Int J Agric & Biol Eng, 2023; 16(3): 143–150.

[13] González-Montellano C, Llana D F, Fuentes J M, Ayuga F. Determination of the mechanical properties of corn grains and olive fruits required in DEM simulations. 2011 Louisville, Kentucky, August 7-10, 2011; 1111505.

[14] Li S J, Li D, Yu S. Meso-parameter inversion of constitutive model for rockfill materials based on macro experimental data. Journal of Shandong University of Science and Technology (Natural Science), 2015; 34(5): 20–26. (in Chinese)

[15] Shi L R, Zhao W Y, Sun W, Yang X P, Wang G P, Xin S L. Analysis of the metering performance for typical shape maize seeds using DEM. Int J Agric & Biol Eng, 2023; 16(1): 26–35.

[16] Martin C L, Bouvard D, Shima S. Study of particle rearrangement during powder compaction by the discrete element method. Journal of the Mechanics and Physics of Solids, 2003; 51(4): 667–693.

[17] Santos K G, Campos A V P, Oliveira O S, Ferreira L V, Francisquetti M C, Barrozo M A S. DEM simulations of dynamic angle of repose of acerola residue: A parametric study using a response surface technique. XX Congresso Brasileiro de Engenharia Química, 2014. doi: 10.5151/chemeng-cobeq2014-0187-26615-184001.

[18] Wang J W, Tang H, Wang J F, Huang H N, Lin N N, Zhao Y. Numerical analysis and performance optimization experiment on hanging unilateral ridger for paddy field. Transactions of the CSAM, 2017; 48(8): 72–80. (in Chinese)

[19] Zhang W X, Wang F Y. Parameter calibration of American ginseng seeds for discrete element simulation. Int J Agric & Biol Eng, 2022; 15(6): 16–22.

[20] Liang R Q, Chen X G, Zhang B C, Wang X Z, Kan Z, Meng H W. Calibration and test of the contact parameters for chopped cotton stems based on discrete element method. Int J Agric & Biol Eng, 2022; 15(5): 1–8.

[21] Yuan J, Li J G, Zou L L, Liu X M. Optimal design of spinach root-cutting shovel based on discrete element method. Transactions of the CSAM, 2020; 51(S2): 85–98. (in Chinese)

[22] Wu T, Huang W F, Chen X S, Ma X, Han Z Q, Pan T. Calibration of discrete element model parameters for cohesive soil considering the cohesion between particles. Journal of South China Agricultural University, 2017; 38(3): 93–98. (in Chinese)

[23] Yan D H. Comparison of moisture content of ginger of different origins and specifications. The 6th Annual Conference of Chinese Pharmaceutical Association, 2006; pp.2172–2175. (in Chinese)

[24] Shi L R, Zhao W Y, Yang X P. Effects of typical corn kernel shapes on the forming of repose angle by DEM simulation. Int J Agric & Biol Eng, 2022; 15(2): 248–255.

[25] Sun J B, Liu Q, Yang F Z, Liu Z J, Wang Z. Calibration of discrete element simulation parameters of sloping soil on loess plateau and its interaction with rotary tillage components. Transactions of the CSAM, 2022; 53(1): 63–73. (in Chinese)

[26] Yao S Q, Shi G K, Wang B S, Peng H J, Meng H W, Kan Z. Calibration of the simulation parameters of jujubes in dwarfing and closer cultivation in Xinjiang during harvest period. Int J Agric & Biol Eng, 2022; 15(2): 256–264.

[27] Li J W, Tong J, Hu B, Wang H B, Mao C Y, Ma Y H. Calibration of parameters of interaction between clayey black soil with different moisture content and soil-engaging component in northeast China. Transactions of the CSAE, 2019; 35(6): 130–140. (in Chinese)

[28] Yu Q X, Liu Y, Chen X B, Sun K, Lai Q H. Calibration and experiment of simulation parameters for panax notoginseng seeds based on DEM. Transactions of the CSAM, 2020; 51(2): 123–132. (in Chinese)

[29] Wang F Y. Production technology and harvesting equipment of green Chinese onion. Agricultural Engineering, 2017; 7(5): 1–4. (in Chinese)

[30] Shi L R, Zhao W Y, Sun B G, Sun W. Determination of the coefficient of rolling friction of irregularly shaped maize particles by using discrete element method. Int J Agric & Biol Eng, 2020; 13(2): 15–25.

[31] Dun G Q, Mao N, Gao Z Y, Wu X P, Liu W H, Zhou C. Model construction of soybean average diameter and hole parameters of seed-metering wheel based on DEM. Int J Agric & Biol Eng, 2022; 15(1): 101–110.

[32] Chen S F, Li Y M, Sun X Z. Research on digging parts of peanut combine harvester. Chinese Agriculture Mechanization, 2005; 1: 47–49. (in Chinese)

[33] Shi L R, Yang X P, Zhao W Y, Sun W, Wang G P, Sun B G. Investigation of interaction effect between static and rolling friction of corn kernels on repose formation by DEM. Int J Agric & Biol Eng, 2021; 14(5): 238–246.

[34] Fu W, Chen H T, Kan Z. Optimizing parameters on vibration break shovel of radish harvester. Transactions of the CSAE, 2011; 27(11): 46–50. (in Chinese)

[35] Hou J L, Chen Y Y, Li Y H, Li T H, Li G H, Guo H E. Design and experiment of shovel-screen combined green onion digging, shaking, and soil tillage device. Transactions of the CSAE, 2021; 37(18): 29–39. (in Chinese)

[36] Zhang P C, Li F G, Wang F Y. Optimization and test of ginger-shaking and harvesting device based on EDEM software. Computers and Electronics in Agriculture, 2023; 213: 108257.

[37] Jia H L, Deng J Y, Deng Y L, Chen T Y, Wang G, Sun Z J, et al. Contact parameter analysis and calibration in discrete element simulation of rice straw. Int J Agric & Biol Eng, 2021; 14(4): 72–81.

[38] Wei Z C, Su G L, Li X Q, Wang F M, Sun C Z, Meng P X. Parameter optimization and test of potato harvester wavy sieve based on EDEM. Transactions of the CSAM, 2020; 51(10): 109–122. (in Chinese)